J Biomol NMR (2013) 56:31–39
DOI 10.1007/s10858-013-9712-3

ARTICLE

# A NMR guided approach for CsrA–RNA crystallization

**Leonardus M. I. Koharudin · Rolf Boelens · Rob Kaptein · Angela M. Gronenborn**

Received: 21 November 2012 / Accepted: 21 January 2013 / Published online: 29 January 2013


**Abstract** Structure determination of protein–nucleic acid complexes remains a challenging task. Here we present a simple method for generating crystals of a CsrA–nucleic acid complex, guided entirely by results from nuclear magnetic resonances spectroscopy (NMR) spectroscopy. Using a construct that lacks thirteen non-essential C-terminal residues, efficient binding to DNA could be demonstrated. One CsrA dimer interacts with two DNA oligonucleotides, similar to previous findings with RNA. Furthermore, the NMR study of the CsrA–DNA complex was the basis for successfully homing in on conditions that were suitable for obtaining crystals of the CsrA–DNA complex. Our results may be useful for those cases where RNA in protein–nucleic acid complexes may be replaced by DNA.

**Keywords** CsrA · NMR spectroscopy · X-Ray crystallography · Protein–RNA complex · RNA binding protein

## Introduction

Crystallization of RNA–protein complexes is possibly the least predictable step in any structure determination project by X-ray crystallography. Many factors inherently affect the crystallizability of any complex, including purity of the components, interaction surface area, conformational heterogeneity, and structural dynamics. Despite many approaches to improve the success rate of obtaining crystals, it is still a daunting task to crystallize a RNA–protein complex, seemingly much more difficult than crystallizing other protein complexes. As an alternative, NMR spectroscopy has been successfully used to study the interactions between RNA and proteins: not only can NMR provide the three dimensional architecture of the complex, it also yields additional information on any conformational changes that are experienced by either the RNA molecule, the protein, or both upon binding (Leulliot and Varani 2001; Williamson 2000). Indeed, large changes in conformation are frequently observed in RNA–protein complex formation. Furthermore, NMR is ideally suited to identify and characterize structured and unstructured regions in biological molecules and their inter-conversions: folding upon binding is generally accepted to play a pivotal role in protein–nucleic acid interactions. Therefore, even without the need to obtain well diffraction crystals, determining solution structures of RNA–protein complexes also remains extremely challenging.

Here we present an NMR guided method for generating crystals of the complex between the protein CsrA and its cognate RNA binding partner. CsrA is a small RNA binding protein (Romeo 1996; Romeo et al. 1993) that is involved in regulating various cellular processes either repressing or activating expression (Yang et al. 1996; Sabnis et al. 1995; Romeo et al. 1993; Jackson et al. 2002; Wei et al. 2000, 2001. In *E. coli*, CsrA's activity is modulated by two non-coding RNAs, CsrB (Liu et al. 1997) and CsrC (Weilbacher et al. 2003) that act by sequestering multiple CsrA dimers (Romeo 1998, 1996; Liu et al. 1997;

L. M. I. Koharudin · A. M. Gronenborn (✉)
Department of Structural Biology, University of Pittsburgh School of Medicine, 3501 Fifth Avenue, BST3/Rm1050, Pittsburgh, PA 15260, USA
e-mail: amg100@pitt.edu

R. Boelens · R. Kaptein
NMR Spectroscopy, Bijvoet Centrum for Biomolecular Research, Utrecht University, 3584 CH Utrecht, The Netherlands

R. Kaptein
Novosibirsk State University, Pirogova 2, 630090 Novosibirsk, Russia

Gudapaty et al. 2001; Baker et al. 2002). Binding to the RNA is mediated by the consensus nucleotide sequence of YAN**GGA**NR, containing a conserved GGA triplet at its center, with Y a pyrimidine nucleotide, R a purine nucleotide, and N any nucleotide (Liu et al. 1997; Baker et al. 2002; Dubey et al. 2003; Weilbacher et al. 2003). A structure of the RsmA homolog of CsrA and its cognate RNA ligand has been reported (Schubert et al. 2007), but no structure of a CsrA complex with either CsrB or CsrC is available. As a first step towards obtaining the crystal structure of the *B. subtilis* CsrA in complex with several different RNA ligands, we generated a different construct of CsrA in which thirteen non-essential residues were deleted from the C-terminus. This CsrA protein construct interacts with DNA, provided that a hairpin is formed, with the consensus GGA triplet located in the loop. An NMR sample of the CsrA–DNA complex was used for crystallization screening. Thus, expensive RNA oligonucleotides could be omitted in the primary large-scale screens for obtaining suitable crystals of the CsrA–RNA complex. Using NMR spectroscopy and crystallization screens in this manner permitted to successfully select conditions that are suitable for preparing crystals of the CsrA–DNA complex. Optimization for improving diffraction quality is in progress and the conditions will also be helpful to generate crystals of the complex between CsrA and ligand RNA.

## Results

### ΔC-CsrA is a superior protein construct than full length CsrA

We previously investigated full-length *B. subtilis* CsrA that contains of 74 residues (White et al. 1996) (Fig. 1a). As can be deduced from the 2D $^{1}H$–$^{15}N$ HSQC spectrum presented in Fig. 1b, the full-length protein with an additional N-terminal His-tag contains an unstructured C-terminus, as judged by the random coil $^{1}H_N$, $^{15}N$ and $^{13}C$ chemical shift values for these residues (Wishart et al. 1992). This is also confirmed by the $^{1}H$–$^{15}N$ het-NOE relaxation data (Fig. 1c). In order to minimize any detrimental influences of flexible regions at the N- and C-termini of the protein for the NMR investigation and crystallization of the protein-RNA complex, we created a new protein construct in which 13 residues were deleted from the C-terminus. In addition, the N-terminus was modified by re-cloning into a pET-15b plasmid. The new construct (designated ΔC-CsrA) contains 64 amino acids, 61 residues of native protein sequence with three additional N-terminal residues remaining after thrombin cleavage of the His-tag. The 2D $^{1}H$–$^{15}N$ HSQC spectrum of this protein construct (Fig. 1d) exhibits well dispersed and narrow resonances, indicative of a native, folded structure. Backbone resonance assignments were carried out based on standard triple resonance NMR data.

### ΔC-CsrA binds to hairpin but not linear DNAs

The SELEX-derived RNA consensus sequence that is critical for CsrA binding was determined as RUACARG GAUGU (Dubey et al. 2005). Figure 2a shows the predicted structure of one such selected high-affinity RNA ligand with a linear sequence of 5′-UAGCACAA**GGA**UG UGCAUA-3′. Note that the bolded GGA triplet has been reported to be pivotal for recognition by the CsrA protein (Liu et al. 1997; Baker et al. 2002; Dubey et al. 2003; Weilbacher et al. 2003).

In an attempt to minimize the costs for CsrA–RNA crystallization trials we tested whether CsrA also recognizes DNA oligonucleotides. The first two DNA oligonucleotides tested were 5′-GCACAA**GGA**TGTGC-3′ (designated CsrADNA1; Table 1; Fig. 2b) and 5′-GATA TAA**GGA**AAAGAG-3′ (designated CsrADNA2; Table 1; Fig. 2c). The first sequence was selected to mimic the high affinity SELEX-derived RNA ligand, while the second sequence was created to elucidate whether CsrA may also recognize a linear nucleic acid, containing the GGA consensus sequence. The 1D $^{1}H$ spectra of the imino proton region of these two DNA oligos confirmed that the first DNA oligo forms a hairpin structure, while the second oligo is mainly linear, with no imino resonances observable in the relevant region of the spectrum (even at 7 °C). For the hairpin oligonucleotide, assignments of the imino resonances were completed using the 2D $^{1}H$–$^{1}H$ NOESY spectra, recorded at 7 °C (Fig. 2e).

Titration experiments with CsrA revealed that the protein only interacts with the hairpin DNA oligonucleotide, but not the linear one. As shown in Fig. 2f, all imino signals of the hairpin oligonucleotide were perturbed upon addition of one molar equivalent of CsrA. Interestingly, we also did not observe additional imino signals, indicating that the consensus GGA triplet is not forming additional hydrogen bonds via their imino groups. In contrast, no changes in chemical shifts were noted when the linear DNA oligonucleotide was titrated with the same amount of protein (data not shown).

### Both hairpin structure and the GGA triplet are critical for recognition by CsrA

In order to further delineate the binding specificity of CsrA, we changed each base within the consensus GGA triplet and carried out titration experiments. Four additional hairpin DNA oligos (5′-CCGCACAA**GGA**TGTGCGG-3′, 5′-CCGCACAA**AGA**TGTGCGG-3′, 5′-CCGCACAA**GA A**TGTGCGG-3′ and 5′-CCGCACAA**AAA**TGTGCGG-3′,

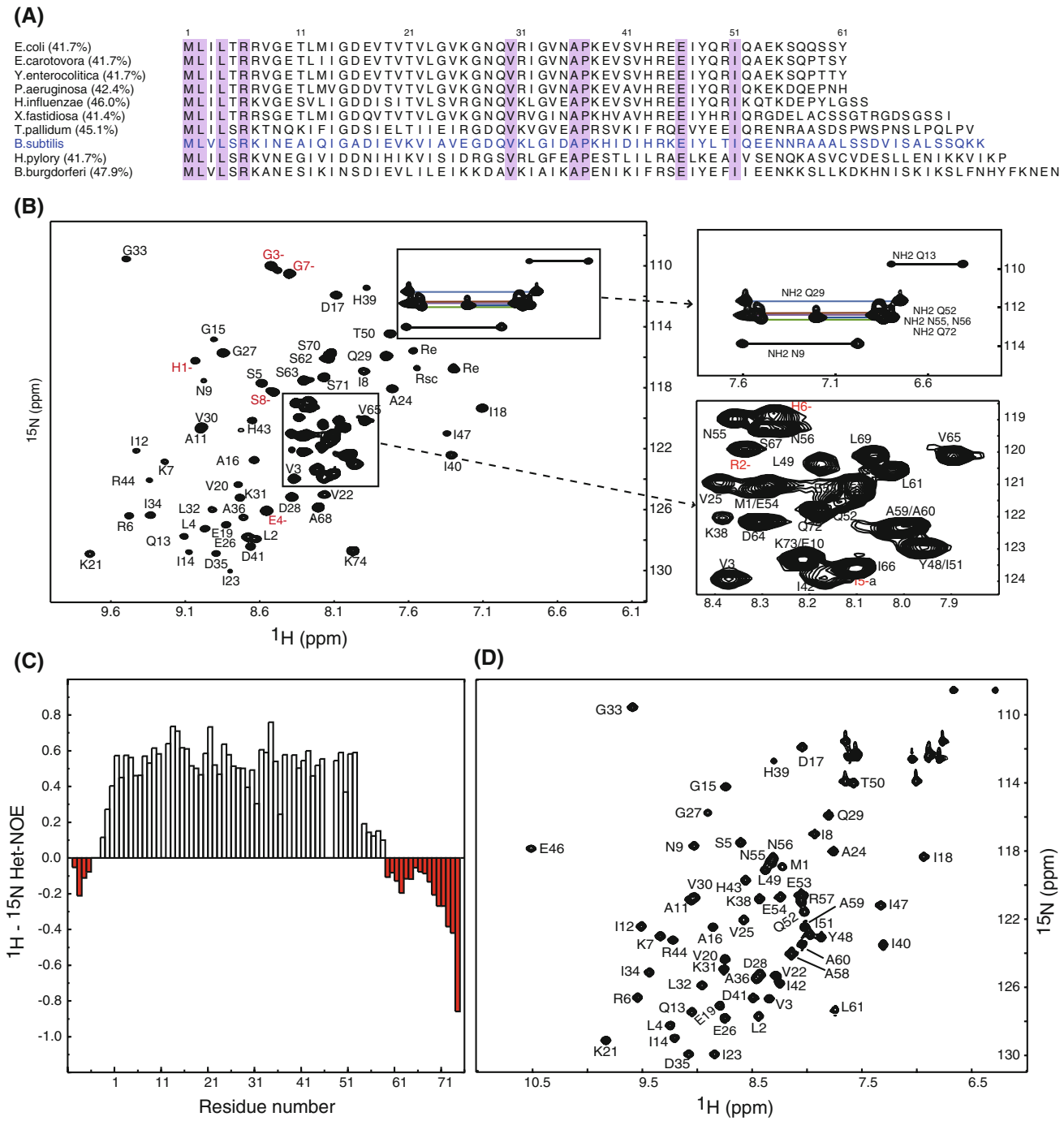


**Fig. 1** Amino acid sequence and 2D $^{1}H$–$^{15}N$ HSQC spectrum of *B. subtilis* CsrA. **a** Amino acid sequence alignment for several bacterial CsrA. Completely conserved residues are highlighted in *magenta boxes*. The sequence of *B. subtilis* CsrA is depicted in blue. Sequence identities with respect to the *B. subtilis* CsrA sequence are given in *brackets*. **b** The 2D $^{1}H$–$^{15}N$ HSQC spectrum of full length CsrA. The spectrum was recorded on a 0.5 mM protein sample at 27 °C in 50 mM NaPhosphate buffer, 150 mM NaCl, pH 5.2. The *inset* at the top shows the side chain resonance assignments of Gln and Asn, while the lower region mainly contains resonances for the flexible C-terminal residues of CsrA. **c** Steady state $^{1}H$–$^{15}N$ heteronuclear NOEs of full length CsrA. Spectral overlap is indicated by the absence of a bar (E10), and very weak resonances (K45 and E46) are also omitted. Note that the P37 residue does not possess an amide resonances. **d** The 2D $^{1}H$–$^{15}N$ HSQC spectrum of ΔC-CsrA. The spectrum was recorded on an ~1.0 mM protein sample at 25 °C in 20 mM NaAcetate (pH 5.0), 20 mM NaCl, 3 mM $NaN_3$, and 90/10 % $H_2O/D_2O$

designated as CsrADNA3, CsrADNA4, CsrADNA5 and CsrADNA6 were investigated (Table 1). In order to assess the interaction for crystallization screening purposes, we performed titrations by monitoring the 2D $^{1}H$–$^{15}N$ HSQC spectrum of CsrA and followed resonances that were affected by the addition of DNA oligonucleotides.

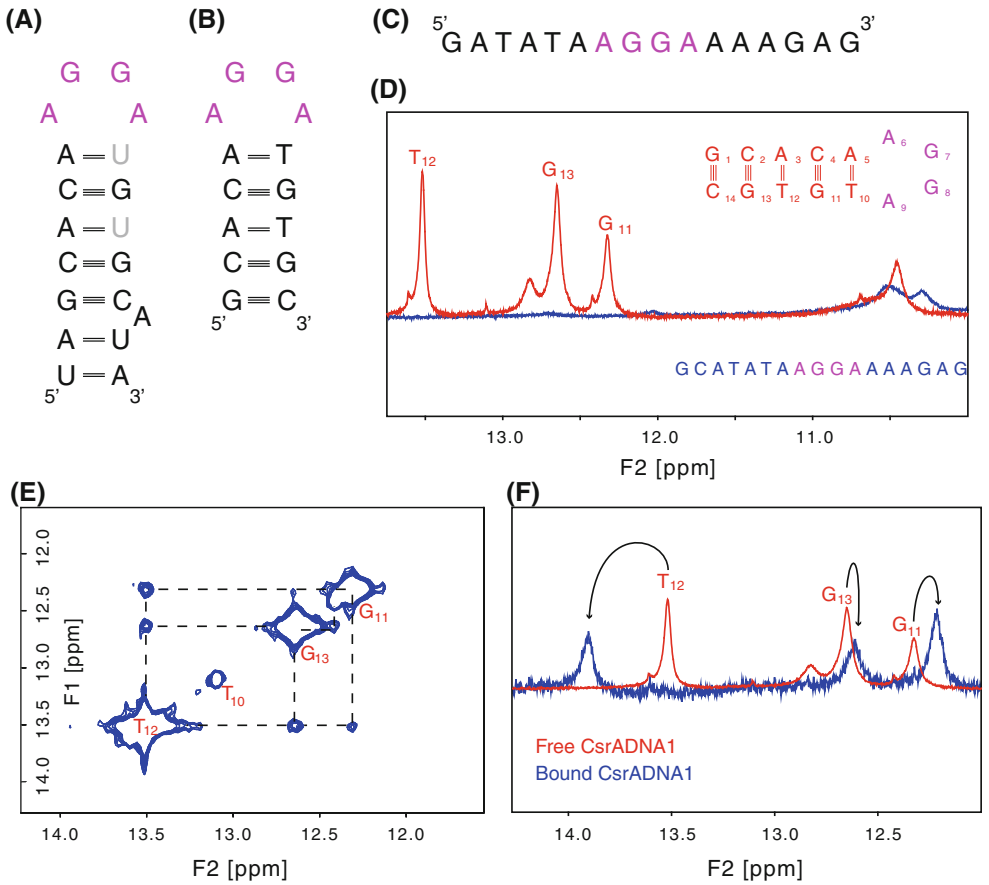


**Fig. 2** Sequence, secondary structure, and 1D $^{1}$H spectra of CsraDNA1 and CsrADNA2 oligonucleotides. **a** Consensus sequence (5′-UAGCACAA**GGA**UGUGCAUA-3′) and the predicted secondary structure of a selected high-affinity RNA ligand based on SELEX result. **b**, **c** Sequences and secondary structures of CsrADNA1 and CsrADNA2 oligonucleotidess. Note, both DNA oligonucleotides contain the consensus GGA triple in the middle of the sequences. **d** 1D $^{1}$H NMR spectra of the imino region of CsrADNA1 (*red*) and CsrADNA2 (*blue*) at 25 °C in 20 mM NaAcetate (pH 5.0), 20 mM NaCl, 3 mM $NaN_3$, and 90/10 % $H_2O/D_2O$. The absence of imino resonances for the CsrADNA2 oligonucleotide indicates that this molecule is without stable secondary structure. **e** The expanded imino region of the 2D $^{1}$H–$^{1}$H NOESY spectrum of CsrADNA1 at 7 °C used for the assignment of the resonances. Every resonance has been assigned, except that for G1 that could not be detected, possibly due to fraying at the ends of the hairpin. **f** The 1D $^{1}$H spectra of CsraDNA1 in the absence (*red*) and the presence (*blue*) of one molar equivalent of ΔC-CsrA, recorded at 25 °C in 20 mM NaAcetate (pH 5.0), 20 mM NaCl, 3 mM $NaN_3$, and 90/10 % $H_2O/D_2O$. Note, all imino resonances experience chemical shift perturbations, confirming that ΔC-CsrA interacts with the majority of the stem-loop structure

Figure 3 displays superpositions of the 2D $^{1}$H–$^{15}$N HSQC spectra of $^{15}$N-labeled ΔC-CsrA dimer in the absence (colored in black) and the presence of ∼2.50 fold molar excess the DNA hairpin oligonuclotide (different colors are used for the different oligos). Note that titrations experiments were carried out in order to determine the stoichiometry between protein and DNA. As can easily be appreciated, the majority of CsrA resonances are affected by the CsrADNA3 oligo (colored in red, Fig. 3a). This demonstrates that CsrA interacts tightly and specifically with CsrADNA3, with one CsrA dimer binding to two molecules of DNA. No perturbations of the CsrA spectra were observed when CsrADNA4 (colored in blue, Fig. 3b), CsrADNA5 (colored in green, Fig. 3c) or CsrADNA6 (colored in magenta, Fig. 3d) were added to the protein sample, indicating that no interaction between CsrA and any of these three oligonucleotides occurs. Given the above titration results, it is evident that CsrA binding requires both the consensus GGA triplet and a hairpin structure in the oligonucleotide for binding.

## Crystallization trials of CsrA–DNA complex

Based on the results of the NMR titrations, we succeeded to prepare a solution of CsrA–CsrADNA3 complex in which all protein is completely bound by DNA. This sample was subsequently used for crystallization screening using over 400 different precipitant conditions. The protein concentration in the complex after the final addition of DNA is ∼7 mg/mL. As shown in Fig. 4, two different conditions yielded crystals of the CsrA–DNA complex. The first condition generated individual cube-like crystals, while the

**Table 1** DNA oligonucleotides used in this study

| Name | Sequence | Shape | Figure |
|---|---|---|---|
| CsrADNA1 | GGCACA AGGA TGTGCC | Hairpin |  |
| CsrADNA2 | GATATA AGGA AAAGAG | Linear | 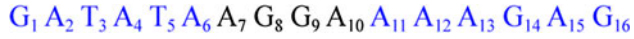 |
| CsrADNA3 | CCGGCACA AGGA TGTGCCGG | Hairpin | 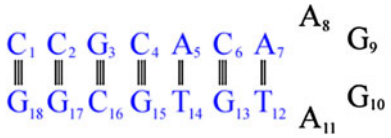 |
| CsrADNA4 | CCGGCACA AAGA TGTGCCGG | Hairpin |  |
| CsrADNA5 | CCGGCACA AGAA TGTGCCGG | Hairpin |  |
| CsrADNA6 | CCGGCACA AAAA TGTGCCGG | Hairpin | 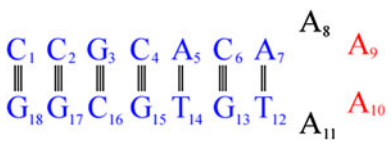 |

second condition generated clusters of thin needles. Both types of crystals were tested for diffraction, and at present resolution up to ~4 Å is observed, most likely due to high solvent content and un-optimized cryo conditions. Therefore, optimization strategies are clearly necessary for improving the diffraction quality for these CsrA–DNA crystals. Although the NMR titration experiments represent additional steps prior to crystallization trials, they clearly enabled us to isolate a suitable complex in obtaining crystals.

## Discussion

The structures of *E. coli* (Gutierrez et al. 2005) and *P. aeruginosa* (Rife et al. 2005) CsrA as well as of the *Y. enterocolitica* homolog, RsmA (Heeb et al. 2006) were previously determined by either NMR spectroscopy or X-ray crystallography. Interestingly, all structures exhibit domain swapping via an exchange of the first β strand between the two monomers. In addition, a structure of the complex between RsmA and its cognate RNA ligand is also available (Schubert et al. 2007). In the latter, two molecules of RNA are bound per molecule of RmsA. In our pursuit to obtain crystallographic structures of *B. subtilis* CsrA complexed with several different RNA ligands, we devised an alternative method to the commonly used crystallization matrix screening: we employed NMR spectroscopy to discover suitable crystallization conditions. Based on our NMR results, we established that (1) a stem-loop structure with the consensus GGA triplet in the loop are essential for tight and specific binding by CsrA and (2) that one CsrA dimer binds to two molecules of nucleic acid, similar to what is seen in the RsmA/RNA crystal structure (Schubert et al. 2007). As a preliminary step, we have recently carried out titration experiments between ΔC-CsrA and an RNA oligonucleotide (5′-rCrCrGrGrCrA rCrArArGrGrA-rUrGrUrGrCrCrGrG-3′, termed as CsrAR NA3; the RNA equivalent of CsrADNA3). As shown in Fig. 4c, ΔC-CsrA indeed binds to CsrARNA3 as demonstrated by chemical shift perturbation of CsrA resonances. In addition, we also confirmed the interaction by monitoring chemical shift perturbation of the RNA imino proton resonances (inset in Fig. 4c). As for the DNA, the binding

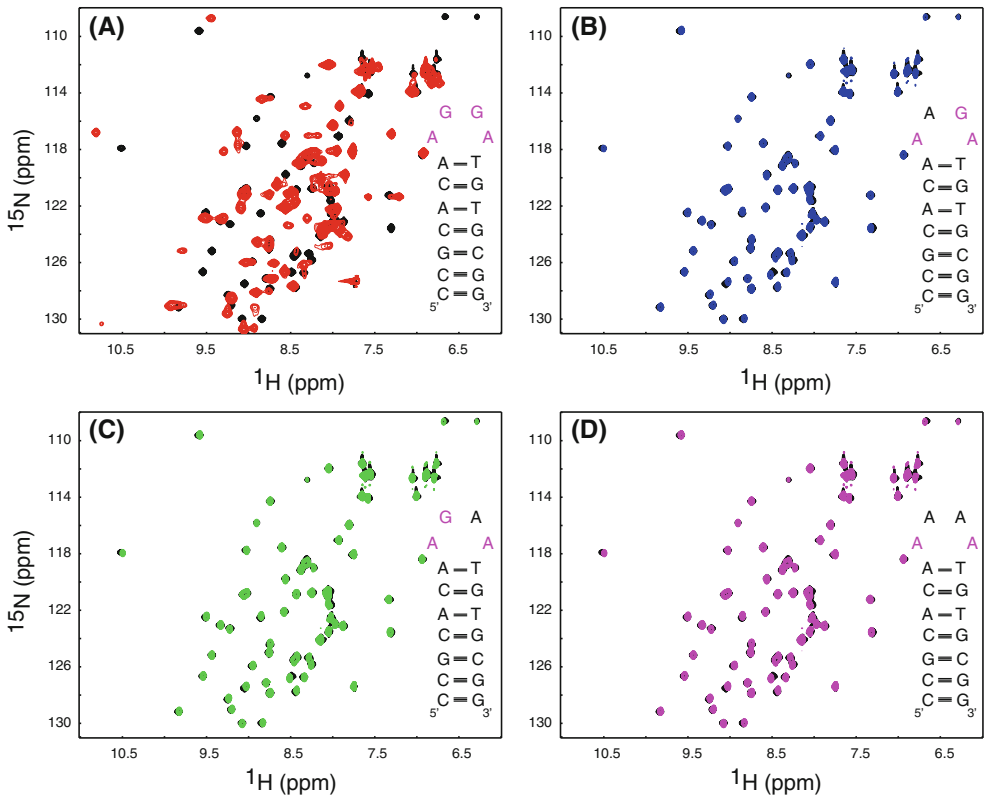


**Fig. 3** Chemical shift perturbations observed in titrations of ΔC-CsrA with various DNA hairpins. (**a**)–(**d**) Superpositions of 2D $^{1}$H–$^{15}$N spectra of nucleotide-free ΔC-CsrA (*black*) and bound ΔC-CsrA in the presence of ~2.5 molar equivalents of CsrADNA3 (*red*) (**a**), in the presence of ~2.5 molar equivalents of CsrADNA4 (*blue*) (**b**), in the presence of ~2.5 molar equivalents of CsrADNA5 (*green*) (**b**), and in the presence of ~2.5 molar equivalents of CsrADNA6 (*magenta*) (**d**). Note, all spectra were recorded at a protein concentration of ~14 mg/mL in 20 mM NaAcetate (pH 5.0), 20 mM NaCl, 3 mM $NaN_3$, and 90/10 % $H_2O/D_2O$ at 25 °C and titrations experiments were carried out in order to determine the stoichiometry between protein and DNA. It is evident that ΔC-CsrA interacts only with CsrADNA3 (**a**) as indicated by perturbation of almost all signals of the protein. Note, that based on the titration results, binding is in slow exchange on the chemical shift scale and that the stoichiometry of CsrA dimer:DNA is 1:2

stoichiometry between ΔC-CsrA and the RNA oligo is 1:2 (CsrA dimer:RNA oligo), confirming previous observation by Schubert and colleagues (Schubert et al. 2007). Taken together, our NMR studies clearly provided major information for obtaining crystals between CsrA and RNA in the future: First, we were able to identify unstructured, flexible regions in the protein that, in the past, prohibited crystallization, thereby guiding us in the creation of new constructs that promote easy crystallization of this relatively small protein. Second, it was possible to replace expensive RNA oligonucleotides with less expensive DNA oligonucleotides, in the initial studies aimed at delineating the RNA binding specify of CsrA using NMR. While this strategy may not be applicable for all RNA binding proteins, it is an easy and cost-effective way, provided that DNA oligonucleotides of equivalent sequence and secondary structural characteristics are employed in such studies. Third, our NMR titration results also guided us towards optimal conditions for complex formation, resulting in obtaining crystals. As a result of our extensive NMR screening, we have now obtained preliminary crystals of the CsrA–DNA complex. Starting from these conditions we currently are extending our crystallization screening to CsrA–RNA complexes.

## Materials and methods

### Expression and purification of ΔC-CsrA

The gene encoding ΔC-CsrA was amplified using the full length CsrA gene in the pET-16b vector (Novagen) as a template. Primers for the polymerase chain reaction (PCR) reaction were 5′-CCCAAACATATGCTAGTTTTATCG CGGAAAATAAACGAAGCGATTC-3′ and 5′-GGGTT TCTCGAGTTATAACGCTGCTGCACGGTTATTTTCT TCC-3′ as forward and reverse primers, respectively. The amplified product was then cloned into the pET-15b expression vector (Novagen), using NdeI and XhoI restriction sites at the 5′ and 3′ ends, respectively. This

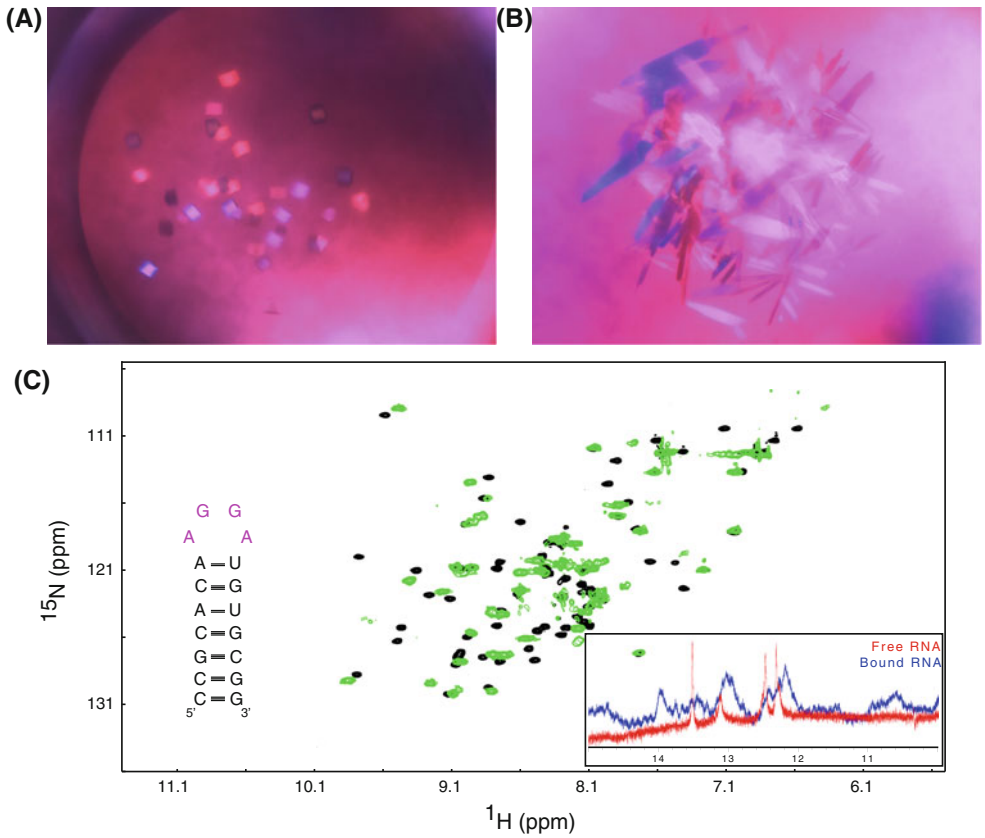


**Fig. 4** Crystallization results for the CsrA–DNA complex and formation of the CsrA–RNA complex. Crystals of the ΔC-CsrA–CsrADNA3 complex, obtained in 1.0 mM spermine, 20 mM magnesium chloride, 1.0 mM cobalt(III)hexaammine chloride, 0.05 M sodium cacodylate (pH 7.0) and 15 % ethanol (**a**) and in 0.2 M sodium acetate trihydrate (pH 4.6) and 2.0 M ammonium sulphate (**b**). (**c**) Superposition of 2D $^{1}$H–$^{15}$N spectra of RNA-free (*black*) and RNA-bound ΔC-CsrA in the presence of ~2.0 molar equivalents of RNA oligonucleotide (CsrARNA3; in *green*). Spectra were recorded at a protein concentration of 0.1 mM in 20 mM NaAcetate (pH 5.0), 20 mM NaCl, 3 mM $NaN_3$, and 90/10 % $H_2O/D_2O$ at 35 °C. In the *inset*, the 1D $^{1}$H spectra of 0.1 mM CsrARNA3 in the absence (*red*) and the presence (*blue*) of excess ΔC-CsrA are provided. The 1D spectra were recorded at 35 °C with the RNA dissolved in 20 mM NaAcetate (pH 5.0), 20 mM NaCl, 3 mM $NaN_3$, and 90/10 % $H_2O/D_2O$

procedure generates an N-terminal His-tagged ΔC-CsrA with 3 additional residues (Gly-Ser-His) at the N-terminus after thrombin cleavage.

For protein expression, *E. coli* Rosetta2 (DE3) cells (Novagen) were transformed with pET-15b-ΔC-CsrA vector. Cells were initially grown at 37 °C, induced with 1 mM IPTG, and grown for ~18 h at 16 °C for protein expression. Isotopic labeling was carried out by growing the cultures in modified M9 minimal media, supplemented with $^{15}$N-labeled $NH_4Cl/^{12}$C-glucose or with $^{15}$N-labeled $NH_4Cl/^{13}$C-labeled glucose as the sole nitrogen and/or carbon sources, respectively.

The over-expressed his-tagged ΔC-CsrA protein was isolated using a three-step standard purification procedure. After sonification of the cells the cell debris was removed by centrifugation and the supernatant was filtered through a 0.45 μm filter and loaded onto a $Ni^{2+}$ affinity column (GE Healthcare). The protein was eluted using a linear gradient of imidazole (20–500 mM), followed by thrombin digestion and dialysis in 20 mM Tris–HCl buffer (pH 8.0) and 100 mM NaCl. After cleavage, the protein was subjected to gel filtration using Superdex75 (GE Healthcare) in 20 mM Tris–HCl buffer (pH 8.0), 100 mM NaCl, 1 mM DTT, 0.02 % $NaN_3$. The final purification involved another step of ion exchange chromatography on a SP(HP) column (GE Healthcare) using a linear gradient of NaCl (0–1,000 mM) for elution. Fractions containing pure protein were collected and concentrated by ultrafiltration using centriprep devices (MW cut-off 3 kDa—Millipore) up to ~14 mg/mL with simultaneous buffer exchange to 20 mM NaAcetate, 3 mM $NaN_3$, 90/10 % $H_2O/D_2O$ (pH 5.0) for both crystallization and NMR studies. The dimeric state of the protein was assessed by size-exclusion chromatography in conjunction with in-line multi-angle light scattering and refractive index detection. Note that the measurement for protein concentration was based on the calculated molar extinction coefficient of 1,280 $M^{-1}$ $cm^{-1}$ (Expasy).

### DNA and RNA preparation

All DNA and RNA oligonucleotides were purchased from Integrated DNA Technology (USA). Each oligonucleotide was treated carefully to encourage stem-loop formation in its monomeric state by incubation at 90 °C for 2 min and rapid cooling by plunging into ice. The molecular masses and quaternary state of the DNA oligos were confirmed by size-exclusion chromatography in conjunction with in-line multi-angle light scattering and refractive index detection.

### Nuclear magnetic resonances spectroscopy

3D HNCACB and CBCA(CO)NH spectra (Bax and Grzesiek 1993) were recorded for complete backbone chemical shift assignment of apo ΔC-CsrA at 25 °C on a Bruker AVANCE800 spectrometer, equipped with a 5 mm triple-resonance, *z*-axis gradient cryoprobe. The protein spectra were recorded on a $^{13}C/^{15}N$-labeled sample (~1.0 mM) in 20 mM NaAcetate, 20 mM NaCl, 3 mM $NaN_3$, 90/10 % $H_2O/D_2O$ (pH 5.0). All spectra were processed with NMRPipe (Delaglio et al. 1995) and analyzed using NMRView (Johnson and Blevins 1994).

Titration experiments were used to monitor chemical shift perturbation of protein resonances upon addition of DNA oligonucleotides using $^{15}N$-labeled samples (14 mg/mL). 2D $^{1}H$–$^{15}N$ HSQC spectra after each addition were recorded at 25 °C on a Bruker AVANCE600 spectrometer, equipped with a 5 mm triple-resonance, *z*-axis gradient cryoprobe. For monitoring the chemical shift perturbation of the DNA imino resonances, 1D $^{1}H$ spectra of the oligonucleotides using watergate sequence for water suppression (Piotto et al. 1992) were recorded in the absence and presence of protein. For titrations of CsrA with the RNA oligo, 2D $^{1}H$–$^{15}N$ HSQC spectra were recorded on 0.1 mM $^{15}N$-labeled dimer in the presence of 0, 0.1 and 0.2 mM of RNA. In addition, 1D $^{1}H$ spectra of the RNA were recorded in the absence and presence of protein to map the chemical shift perturbation on the RNA imino resonances.

### Crystallization of the ΔC-CsrA–CsrADNA3 complex

Crystallization trials of the CsrA–DNA complex were carried out by sitting drop vapor diffusion at 4 °C using the NMR titration sample of ΔC-CsrA and CsrADNA3, in which the protein was saturated with ~2.5 molar fold of DNA. Crystallization drops consisted of 2 μL protein and 2 μL of reservoir solutions. Crystals were obtained either in 1.0 mM spermine, 20 mM magnesium chloride, 1.0 mM cobalt(III)hexaammine chloride, 0.05 M sodium cacodylate (pH 7.0) and 15 % ethanol, or in 0.2 M sodium acetate trihydrate (pH 4.6) and 2.0 M ammonium sulphate after ~2–3 weeks. Optimization for improving the diffraction quality of the crystals is currently in process.

**Acknowledgments** The authors thank Mike Delk for NMR technical support.

**Conflict of interest** The authors declare that they have no competing financial interests.

## References

Baker CS, Morozov I, Suzuki K, Romeo T, Babitzke P (2002) CsrA regulates glycogen biosynthesis by preventing translation of glgC in *Escherichia coli*. Mol Microbiol 44(6):1599–1610

Bax A, Grzesiek S (1993) Methodological advances in protein NMR. Acc Chem Res 26(4):131–138

Delaglio F, Grzesiek S, Vuister GW, Zhu G, Pfeifer J, Bax A (1995) Nmrpipe—a multidimensional spectral processing system based on unix pipes. J Biomol NMR 6(3):277–293

Dubey AK, Baker CS, Suzuki K, Jones AD, Pandit P, Romeo T, Babitzke P (2003) CsrA regulates translation of the *Escherichia coli* carbon starvation gene, cstA, by blocking ribosome access to the cstA transcript. J Bacteriol 185(15):4450–4460

Dubey AK, Baker CS, Romeo T, Babitzke P (2005) RNA sequence and secondary structure participate in high-affinity CsrA–RNA interaction. RNA 11(10):1579–1587. doi:10.1261/rna.2990205

Gudapaty S, Suzuki K, Wang X, Babitzke P, Romeo T (2001) Regulatory interactions of Csr components: the RNA binding protein CsrA activates csrB transcription in *Escherichia coli*. J Bacteriol 183(20):6017–6027

Gutierrez P, Li Y, Osborne MJ, Pomerantseva E, Liu Q, Gehring K (2005) Solution structure of the carbon storage regulator protein CsrA from *Escherichia coli*. J Bacteriol 187(10):3496–3501. doi:10.1128/JB.187.10.3496-3501.2005

Heeb S, Kuehne SA, Bycroft M, Crivii S, Allen MD, Haas D, Camara M, Williams P (2006) Functional analysis of the post-transcriptional regulator RsmA reveals a novel RNA-binding site. J Mol Biol 355(5):1026–1036. doi:10.1016/j.jmb.2005.11.045

Jackson DW, Suzuki K, Oakford L, Simecka JW, Hart ME, Romeo T (2002) Biofilm formation and dispersal under the influence of the global regulator CsrA of *Escherichia coli*. J Bacteriol 184(1):290–301

Johnson BA, Blevins RA (1994) NMRView—a computer-program for the visualization and analysis of nmr data. J Biomol NMR 4(5):603–614

Leulliot N, Varani G (2001) Current topics in RNA-protein recognition: control of specificity and biological function through induced fit and conformational capture. Biochemistry 40(27):7947–7956

Liu MY, Gui G, Wei B, Preston JF 3rd, Oakford L, Yuksel U, Giedroc DP, Romeo T (1997) The RNA molecule CsrB binds to the global regulatory protein CsrA and antagonizes its activity in *Escherichia coli*. J Biol Chem 272(28):17502–17510

Piotto M, Saudek V, Sklenar V (1992) Gradient-tailored excitation for single-quantum NMR spectroscopy of aqueous solutions. J Biomol NMR 2(6):661–665

Rife C, Schwarzenbacher R, McMullan D, Abdubek P, Ambing E, Axelrod H, Biorac T, Canaves JM, Chiu HJ, Deacon AM, DiDonato M, Elsliger MA, Godzik A, Grittini C, Grzechnik SK, Hale J, Hampton E, Han GW, Haugen J, Hornsby M, Jaroszewski L, Klock HE, Koesema E, Kreusch A, Kuhn P, Lesley SA, Miller MD, Moy K, Nigoghossian E, Paulsen J, Quijano K,

Reyes R, Sims E, Spraggon G, Stevens RC, van den Bedem H, Velasquez J, Vincent J, White A, Wolf G, Xu Q, Hodgson KO, Wooley J, Wilson IA (2005) Crystal structure of the global regulatory protein CsrA from *Pseudomonas putida* at 2.05 A resolution reveals a new fold. Proteins 61(2):449–453. doi:10.1002/prot.20502

Romeo T (1996) Post-transcriptional regulation of bacterial carbohydrate metabolism: evidence that the gene product CsrA is a global mRNA decay factor. Res Microbiol 147(6–7):505–512

Romeo T (1998) Global regulation by the small RNA-binding protein CsrA and the non-coding RNA molecule CsrB. Mol Microbiol 29(6):1321–1330

Romeo T, Gong M, Liu MY, Brun-Zinkernagel AM (1993) Identification and molecular characterization of csrA, a pleiotropic gene from *Escherichia coli* that affects glycogen biosynthesis, gluconeogenesis, cell size, and surface properties. J Bacteriol 175(15):4744–4755

Sabnis NA, Yang H, Romeo T (1995) Pleiotropic regulation of central carbohydrate metabolism in *Escherichia coli* via the gene csrA. J Biol Chem 270(49):29096–29104

Schubert M, Lapouge K, Duss O, Oberstrass FC, Jelesarov I, Haas D, Allain FH (2007) Molecular basis of messenger RNA recognition by the specific bacterial repressing clamp RsmA/CsrA. Nat Struct Mol Biol 14(9):807–813. doi:10.1038/nsmb1285

Wei B, Shin S, LaPorte D, Wolfe AJ, Romeo T (2000) Global regulatory mutations in csrA and rpoS cause severe central carbon stress in *Escherichia coli* in the presence of acetate. J Bacteriol 182(6):1632–1640

Wei BL, Brun-Zinkernagel AM, Simecka JW, Pruss BM, Babitzke P, Romeo T (2001) Positive regulation of motility and flhDC expression by the RNA-binding protein CsrA of *Escherichia coli*. Mol Microbiol 40(1):245–256

Weilbacher T, Suzuki K, Dubey AK, Wang X, Gudapaty S, Morozov I, Baker CS, Georgellis D, Babitzke P, Romeo T (2003) A novel sRNA component of the carbon storage regulatory system of *Escherichia coli*. Mol Microbiol 48(3):657–670

White D, Hart ME, Romeo T (1996) Phylogenetic distribution of the global regulatory gene csrA among eubacteria. Gene 182(1–2):221–223

Williamson JR (2000) Induced fit in RNA-protein recognition. Nat Struct Biol 7(10):834–837. doi:10.1038/79575

Wishart DS, Sykes BD, Richards FM (1992) The chemical shift index: a fast and simple method for the assignment of protein secondary structure through NMR spectroscopy. Biochemistry 31(6):1647–1651

Yang H, Liu MY, Romeo T (1996) Coordinate genetic regulation of glycogen catabolism and biosynthesis in *Escherichia coli* via the CsrA gene product. J Bacteriol 178(4):1012–1017